



**HAL**  
open science

## Quantum Dot-Based Nanosensors for in Vitro Detection of Mycobacterium Tuberculosis

Viktor V Nikolaev, Tatiana B Lepehina, Alexander S Alliluev, Elham Bidram, Pavel M Sokolov, Igor R Nabiev, Yury V Kistenev

► **To cite this version:**

Viktor V Nikolaev, Tatiana B Lepehina, Alexander S Alliluev, Elham Bidram, Pavel M Sokolov, et al.. Quantum Dot-Based Nanosensors for in Vitro Detection of Mycobacterium Tuberculosis. 2024. hal-04687195

**HAL Id: hal-04687195**

**<https://hal.science/hal-04687195v1>**

Preprint submitted on 4 Sep 2024

**HAL** is a multi-disciplinary open access archive for the deposit and dissemination of scientific research documents, whether they are published or not. The documents may come from teaching and research institutions in France or abroad, or from public or private research centers.

L'archive ouverte pluridisciplinaire **HAL**, est destinée au dépôt et à la diffusion de documents scientifiques de niveau recherche, publiés ou non, émanant des établissements d'enseignement et de recherche français ou étrangers, des laboratoires publics ou privés.

# Quantum Dot–Based Nanosensors for *in Vitro* Detection of *Mycobacterium Tuberculosis*

Viktor V. Nikolaev <sup>1</sup>, Tatiana B. Lepehina <sup>1</sup>, Alexander S. Alliluev <sup>1</sup>, Elham Bidram <sup>2</sup>, Pavel M. Sokolov <sup>3,4,5</sup>, Igor R. Nabiev <sup>3,4,5,6,\*</sup> and Yury V. Kistenev <sup>1,\*</sup>

<sup>1</sup> Laboratory of Laser Molecular Imaging and Machine Learning, National Research Tomsk State University, 36 Lenin av., 634050 Tomsk, Russia; yuk@iao.ru

<sup>2</sup> Department of Biomaterials, Nanotechnology and Tissue Engineering, School of Advanced Technologies in Medicine, Isfahan University of Medical Sciences, Isfahan, Iran; elhambidram@gmail.com

<sup>3</sup> Life Improvement by Future Technologies (LIFT) Center, Skolkovo, 143025 Moscow, Russia; p.sokolov@lift.center

<sup>4</sup> Laboratory of Nano-Bioengineering, National Research Nuclear University MEPhI (Moscow Engineering Physics Institute), 31 Kashirskoe shosse, 115409 Moscow, Russia; socolovpm87@mail.ru

<sup>5</sup> Department of Clinical Immunology and Allergology, Institute of Molecular Medicine, Sechenov First Moscow State Medical University (Sechenov University), 119146 Moscow, Russian Federation

<sup>6</sup> Université de Reims Champagne-Ardenne, Laboratoire BioSpecT (BioSpectroscopie Translationnelle), 51 rue Cognacq Jay, 51100 Reims, France; igor.nabiev@univ-reims.fr

\* Correspondence: [igor.nabiev@univ-reims.fr](mailto:igor.nabiev@univ-reims.fr) (I.R.N.) or [yuk@iao.ru](mailto:yuk@iao.ru) (Yu.V.K.)

**Abstract:** Despite the existing effective treatment methods, tuberculosis (TB) is the second most deadly infectious disease globally, its carriers in the latent and active phases accounting for more than 20% of the world population. An effective method to control TB and reduce the mortality is regular population screening and diagnosis of the latent form of TB in order to take preventive and curative measures. Numerous methods allow diagnosing TB and directly detecting *Mycobacterium tuberculosis* (*M.tb*) biomarkers, including *M.tb* DNA, proteins, and specific metabolites, as well as antibodies produced by the host immune system in response to *M.tb*. PCR, ELISA, immunofluorescence and immunochemical analyses, flow cytometry, and other methods allow the detection of *M.tb* biomarkers or the host immune response to *M.tb* by recording the optical signal of fluorescent or colorimetric dyes included in the diagnostic tools. Current research in biosensors is aimed at increasing the sensitivity of detection, which can be achieved by using brighter and more photostable optical tags containing fluorescent quantum dots. Here, we review current methods for detection of *M.tb* biomarkers using optical sensor systems, primarily quantum dot–based nanosensors, and summarize *M.tb* biomarkers whose detection can be made significantly more sensitive by using quantum dot–based nanosensors.

**Keywords:** quantum dot; nanosensor; tuberculosis; diagnostics

**Citation:** To be added by editorial staff during production.

Academic Editor: Firstname Last-name

Received: date

Revised: date

Accepted: date

Published: date



**Copyright:** © 2024 by the authors. Submitted for possible open access publication under the terms and conditions of the Creative Commons Attribution (CC BY) license (<https://creativecommons.org/licenses/by/4.0/>).

## 1. Introduction

Tuberculosis (TB) is an infectious disease caused by *Mycobacterium tuberculosis* and most often affecting the lungs. In 2022, there were 10.6 million TB cases worldwide, including 5.8 million men, 3.5 million women, and 1.3 million children; a total of 1.3 million people died from TB (including 167,000 people with concomitant HIV infection). Globally, TB is the second leading cause of death among infectious diseases after COVID-19, with death rates higher than those of AIDS [1]. TB can have particularly severe consequences for women, especially those of reproductive age and during pregnancy, and is one of the top five killers of women aged 20–59 years [2]. Recent estimates demonstrate that about 1.7 billion people are latently infected by *M.tb* [3]. At the same time, traditional diagnostic methods, such as chest X-ray and tuberculosis skin tests, do not have a sufficient level of

sensitivity and specificity to reliably diagnose latent forms of TB [4], especially against the background of other diseases or pathological conditions [5]. The risk of progression of latent TB infection to the active form is estimated at 10% [6]. One of the health-related targets of the United Nations Sustainable Development Goals (SDGs) is to end the TB epidemic by 2030 [1]. To attain this goal, it is necessary not only to combat active forms of TB, but also to carry out prevention and therapy for patients with latent TB, which requires methods for diagnosing *M.tb* infection at the earliest stages.

## 2. Current Tuberculosis Diagnostic Methods

TB can be diagnosed in two ways: direct detection of *M.tb* in a clinical specimen or detection of the biomarkers associated with *M.tb* infection. Currently, numerous methods are widely used for TB diagnosis [7–9]. At the moment, there are four major groups of routine clinical methods used for this purpose: rapid molecular diagnostic tests, cultural methods, provocation tests, and diagnosis using optical methods. The characteristics of these groups of methods are presented in Table 1. With exception of skin tests, all the procedures are performed *in vitro*.

**Table 1.** The major groups of routine clinical methods used for tuberculosis diagnosis.

Assay	Biomaterial analyzed	Time of analysis	Advantages	Disadvantages	Sensitivity, specificity	Ref.	Comments
<b>Molecular diagnostic tests</b>							
Polymerase chain reaction (PCR)	Serum, urine, blood, sputum, saliva, lung biopsy samples, BALF, pleural fluid	4–5 h	High specificity, quickness, and informativeness	High cost, limited availability, low sensitivity for non-respiratory samples; detection of DNA only	Sensitivity: 47% (42–51%) Specificity: 95% (93–97%) CrI: 95%	[10]	The sensitivity and specificity are averaged results of 9 studies in 709 subjects
Xpert MTB/RIF Ultra	Raw sputum or concentrated sediment	1.5 h	Detection of <i>rpoB</i> gene mutations associated with rifampicin resistance	High cost	Sensitivity: 89% (85–92%) Specificity: 99% (98–99%) CrI: 95%	[11]	The sensitivity and specificity are averaged result of 22 studies in 8998 subjects, including 2953 confirmed TB cases and 6045 cases without TB
Truenat	Raw sputum	1 h	Use of a portable, chip-based and battery-operated device. Suitability for laboratories with technical equipment	Lower accuracy compared to Xpert MTB/RIF Ultra	Sensitivity: 80% (70.2–88.4%) Specificity: 98% (94.5–99.6%)	[12]	The sensitivity and specificity have been estimated in tests in 250 subjects
LF-LAM	Urine	0.5 h	High efficiency, ease of use, low cost, simple technology, no special equipment. Detection of TB in patients for	Lower sensitivity compared to Xpert MTB/RIF (though higher compared to microscopy methods). Suitability for	Sensitivity: 45% (29–63%) Specificity: 92% (80–97%) CrI: 95%	[13]	The sensitivity and specificity are averaged results of 5 studies in 2313 subjects,

			whom other diagnostic methods cannot be used (e.g., HIV patients)	a limited group of patients only. Impossibility to distinguish <i>M. tb.</i> from other mycobacteria, which requires using other diagnostic methods after the test		including 35% of TB cases	
TB-XT HEMA EX- PRESS	Blood, serum	0.5 h	Quickness, relatively low cost	Low sensitivity, suboptimal performance in the case of high TB prevalence	Sensitivity: 31% (3.9–78%) Specificity: 85% (52–93%)	[14]	The sensitivity and specificity have been estimated in tests in 1386 subjects, including 290 TB cases
<b>TB tests based on T-cells analysis</b>							
IGRA, (T- SPOT.TB, QuantiFERON-TB Gold (QFT))	Blood, serum	up to 2 days	Inensitivity to BCG vaccination or contact with atypical mycobacteria; one-time tests; high efficiency. T-SPOT.TB is less susceptible to immunosuppression and is preferable for the examination of HIV-infected or autoimmunity patients during treatment with immunosuppressants; can be used before starting therapy with biological drugs	Low specificity and sensitivity; high cost; impossibility to distinguish between the active and latent forms of TB and suitability as a primary diagnostic test for LTBI or active TB. The bacterium itself is not determined; the result depends on the state of the patient's immune system	<b>QFT</b> Sensitivity: 66% (47–81%) Specificity: 87% (68–94%) <b>T-SPOT</b> Sensitivity: 60% (48–72%) Specificity: 86% (65–95%)	[15]	The sample consisted of 6,525 HIV-positive patients, including 3,467 TB cases, 806 of them with LTBI and 2,661 with active TB
<b>Cultural methods</b>							
BBL Septi- Chek AFB	Sputum	Up to 23 days	Higher <i>M.tb</i> growth rate compared to methods using an isolated dense medium	Low sensitivity, long time of analysis	Sensitivity: 73% Specificity: 93%	[16]	The sensitivity and specificity have been estimated in studies on 274 specimens
BACTEC (with different parameters of MGIT 460, 960)	Sputum	Up to 14 days	Rapid identification of <i>M.tb</i> and its drug sensitivity; accelerated culture testing of all first-line drugs	High cost, justified only for large laboratories. Semi-automatic monitoring of bacterium growth; many labor-intensive operations; use	<b>MGIT 960</b> Sensitivity: 81.5% Specificity: 99.6% <b>MGIT 460</b>	[17]	The sensitivity and specificity have been estimated in studies on ~8,000 clinical

				of radioisotopes and the need for disposal of radioactive waste; long time of analysis	Sensitivity: 85.8% Specificity: 99.9%		specimens per year. The number after MGIT is the number of wells in the plate.
BacT/ALERT 3D	Sputum	24–72 h	Detection of <i>M.tb</i> growth; detection of <i>M.tb</i> and fungi in blood cultures. Full automation; no radioactive waste	Long time, high cost	Sensitivity: 87.80% Specificity: 99.21%	[18]	The sensitivity and specificity have been estimated in studies on 2659 clinical specimens
<b>Skin tests</b>							
Tuberculin skin tests, Mantoux tests, and Diaskintest ( <i>in vivo</i> )	Skin tests	72 h	Availability; low cost; ease of use	Low specificity and sensitivity; unsuitability for diagnosing active TB forms; false positive results in those who have been infected with <i>M.tb</i> in the past because their memory T cells still secrete interferon; impossibility to distinguish the active and latent forms of TB	Sensitivity: 59% Specificity: 95%	[19]	The sensitivity and specificity have been estimated in tests in 643,694 U.S. Navy recruits
<b>Tests based on mycobacterium staining</b>							
Gabbett's stain, Ziehl–Neelsen stain, modified cold stain (MCS)	Sputum	~24 h	Simplicity, quickness, ease of use, low cost	Low sensitivity and specificity; suitability for pulmonary tuberculosis only; inaccuracy in children and HIV-infected persons; multistage and complex procedure. Impossibility to distinguish between different mycobacteria	<b>Gabbett's stain</b> Sensitivity: 77% Specificity: 98% <b>Ziehl–Neelsen stain</b> Sensitivity: 70% Specificity: 97% <b>MCS</b> Sensitivity: 60% Specificity: 96%	[20]	The sensitivity and specificity have been estimated in tests in 100 patients
Fluorescence microscopy	Sputum	~24 h	Quickness, ease of use, specificity	High cost, frequent burn-out of expensive mercury vapor lamps, need for continuous power supply, need for a dark room	Sensitivity: 72% Specificity: 81%	[21]	The sensitivity and specificity have been estimated in tests in 426 patients
<b>Other methods</b>							

X-ray	Radiographic test	1 h	Quickness	High cost; low specificity	Sensitivity: 96% Specificity: 46%	[22]	The sensitivity and specificity are averaged results of 13 studies
MALDI-TOF MS	BALF, sputum	2.5 h	Rapid, reliable, cost-effective method	Method requires sample preprocessing to generate high-quality proteomic profiles, especially for proteins/peptides or other low-abundance analytes in which MS spectra are obscured by more abundant/high-molecular-weight species. This method is not highly specific because of the matrix proteins and noise issues	Sensitivity: 83%; Specificity: 93%; CrI: 95%	[23]	The sensitivity and specificity have been estimated in tests in 214 patients
LC-MS/MS	Urine, blood	1 h	Proteomic analysis of urine; identification of proteins characteristic of TB	Changes in ionization efficiency in the presence of not only proteins, phospholipids, and salts, but also reagents and contaminants	Sensitivity: 94% Specificity: 100%	[24]	The sensitivity and specificity have been estimated in tests in 57 patients

\* Abbreviations: LF-LAM, lipoarabinomannan lateral shift test; LTBI, latent tuberculosis infection; MGIT, mycobacteria growth indicator tube; IGRA, interferon-gamma release assay; CrI, credible interval; BALF, bronchoalveolar lavage fluid; MALDI-TOF MS, matrix-assisted laser desorption ionization time-of-flight mass spectrometry; LC-MS, liquid chromatography tandem mass spectrometry; MS, mass spectrometry.

### 2.1. Molecular diagnostic tests

Polymerase chain reaction (PCR) is a molecular biology technique based on amplification and further analysis of specific DNA fragments. The amplification involves several cycles of heating and cooling, causing a DNA fragment to be duplicated many times to reach a detectable amount. PCR can detect the presence of a DNA fragment specific for *M.tb* [10]. This method is effective for early TB diagnosis when the number of the microorganisms is insufficient for detection by classical methods. PCR tests also allow analyzing drug resistance of specific *M.tb* strains. The PCR tests have strict requirements for laboratory room purity and personnel skills because their high sensitivity entails their downside

related to the high risk of engaging contaminants in the reaction. PCR tests are suitable for detecting TB sepsis and disseminated TB but not for population screening for TB, where the results could be false negative.

LF-LAM is a lateral flow urine test for diagnosis of TB through the detection of lipoarabinomannan, a mycobacterial cell wall lipoglycan. A disadvantage of the LF-LAM method is its low sensitivity [13]. Because lateral flow tests are cheap and easy to perform, they are often used in diagnosis of TB by detecting IgG antibodies against TB-specific proteins in blood and serum samples [14]. Simultaneous detection of IgG and IgM antibodies has also been reported [25]. In this case, the test band contained a proprietary mixture of recombinant TB antigens that ensured a diagnostic sensitivity of 94.4% in a sample of 125 microbiologically or clinically diagnosed TB patients and a diagnostic specificity of 98.3% in a sample of 400 subjects who were healthy or had respiratory conditions other than TB.

Loop-mediated isothermal amplification (LAMP) uses special primers to amplify DNAs forming loop-shaped intermediates of different sizes, which can be detected using fluorescence measurements or agarose gel electrophoresis [26]. WHO recommends the use of TB-LAMP as a replacement for microscopy for the diagnosis of pulmonary TB [42].

Xpert MTB/RIF Ultra is an improved version of the Xpert MTB/RIF test [28,29]. Xpert MTB/RIF Ultra (*in vitro*) and Truenat can also identify mutations of the *rpoB* gene associated with rifampicin resistance [12,28–30]. Xpert MTB/RIF Ultra and Truenat have a higher sensitivity and a shorter time of analysis than conventional PCR tests.

Serological tests detecting antibodies against specific protein antigens of the recombinant *M.tb* complex have a high specificity but variable sensitivity [14]. The control of multiple *M.tb* complex antigens increases the sensitivity [14]. It should be pointed out that these methods may give false positive results because specific antibodies can occur in the human body for a long time after recovery from TB.

## 2.2. Tuberculosis tests based on T-cell analysis

Interferon-gamma release assay (IGRA) is a group of laboratory tests that evaluate the release of interferon-gamma (INF- $\gamma$ ) by human immune blood cells (T cells) and are performed *in vitro* [15]. There are two different types of blood tests based on this principle approved by FDA: QuantiFERON-TB Gold Plus (QFT) and T-SPOT.TB (T-SPOT). The QFT test is a whole-blood-based enzyme-linked immunosorbent assay (ELISA) measuring the amount of INF- $\gamma$  produced in response to two *M.tb* antigens (ESAT-6 and CFP-10). The T-SPOT test measures the number of T cells that produce INF- $\gamma$  after stimulation with ESAT-6 and CFP-10. These methods may give false positive results because T cells have a long memory of an *M.tb* invasion that might have occurred a long time ago.

## 2.3. Cultural methods

Cultural method remains the gold standard of TB diagnosis confirmation. They consist in inoculation of biological material on solid or liquid differential diagnostic nutrient media for growing mycobacterial colonies. In practice, several cultural methods are used: acid-fast mycobacteria (AFB) [16], BACTEC (with different parameters of MGIT, usually 460 and 960) [31], and BacT/ALERT 3D [18].

The AFB method involves examining human sputum or other samples stained to detect acid-fast bacteria. The latest experimental study using this method dates back to 1997 [31,32], which may be due to the extremely long time of analysis. The sample to be tested is inoculated into one or more vials with a specific growth medium and inserted into the instrument for incubation and periodic fluorescent reading. Each vial contains a chemical sensor detecting an increase in the amount of carbon dioxide produced by the growth of microorganisms. The instrument monitors the sensor every 10 min for an increase in its fluorescence, which is proportional to the amount of CO<sub>2</sub>, a positive reading indicating the presence of viable microorganisms in the vial. BACTEC is a fully automated system not only for *M.tb* detection, but also for the analysis of *M.tb* sensitivity to all the first-line

drugs, including pyrazinamide. BACTEC is a reference method with high sensitivity and specificity, but it takes about 10 days to obtain the result [33]. BacT/ALERT 3D allows automated monitoring the culture medium to detect the growth of microorganisms via monitoring CO<sub>2</sub> release by an increase in reflectance. It has a high sensitivity with a shorter culturing time. BacT and BACTEC have similar operating principles but differ in the details of technology and design.

The key limitation of these methods is a too long time of analysis.

#### 2.4. Skin tests

*In vivo* tuberculin skin tests are based on provocation of the body immune response to TB-associated molecules [19]. For example, the Mantoux test uses a tuberculin solution administered via intradermal injection. All these tests suffer from frequent false positive and false negative results. The point is that the immune system responds to tuberculin if there are mycobacteria in the body, and the majority of people receive the bacteria in the form of the BCG vaccine back in the maternity hospital. Recently, WHO included Diaskintest, which is an advanced and more accurate variant of the Mantoux tuberculin test [34], into the list of recommended TB skin tests.

#### 2.5. Tests based on mycobacterium staining

Staining methods identify acid-fast mycobacteria, actinomycetes, and other acid-fast microorganisms by means of their staining and then analyzing using optical microscopy. These methods differ in the staining solution, which determines the sensitivity and specificity of analysis. The weak point of this group of TB tests is a complex procedure of analysis that requires considerable time and highly skilled personnel.

#### 2.6. Other methods

Chest X-rays are commonly used in the TB diagnosis. They can help identify abnormalities in the lungs that may be indicative of TB infection, such as nodules, cavities, or infiltrates. However, it should be noted that chest X-rays alone cannot definitively diagnose TB.

Matrix-assisted laser desorption/ionization time-of-flight mass spectrometry (MALDI-TOF MS) is based on an ionization technique that allows the ionization of biological macromolecules, such as peptides, proteins, DNA, oligonucleotides, and lipopolysaccharides, in the presence of a special matrix under laser irradiation [35]. Wang et al. [36] have evaluated MALDI-TOF MS as a means of *M.tb* nucleic acid detection for rapid diagnosis of TB and drug resistance. The effectiveness of the MALDI-TOF MS can be improved by using the protocol of destruction of mycobacterium cells and protein extraction [37].

Liquid chromatography–tandem mass spectrometry (LC-MS/MS) is based on coupling mass spectrometers in series to analyze complex mixtures [38]. For example, liquid–liquid extraction and LC-MS analysis were used to determine the pretomanid concentrations in 40 mL of human plasma [39]. The method was proven to be reliable and reproducible for pharmacokinetic analysis of samples in a clinical trial involving TB patients. Another study used the LC-MS technique to detect specific *M.tb* peptides in mouse blood serum. Sixty-five peptides from four recombinant *M.tb* proteins were identified in the mouse blood [40]. This method is not used to directly detect *M.tb*, but it is useful in the monitoring of TB treatment [41].

Figure 1 graphically illustrates the key data from Table 1.



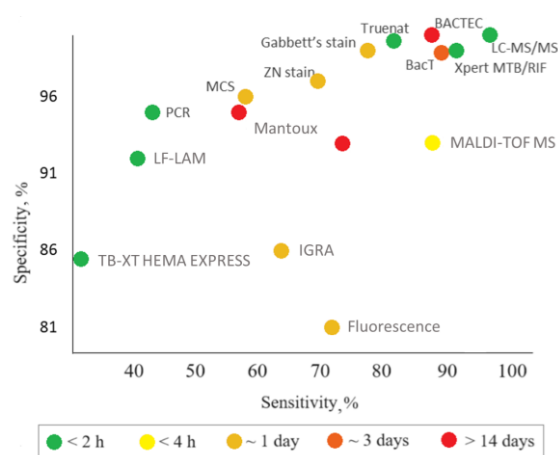


**Figure 1.** Sensitivity and specificity of tuberculosis diagnostic methods shown in Table 1.

Scrutiny of the above TB diagnostic methods shows that all of them have disadvantages and limitations. Therefore, development of new simple and effective methods of TB diagnosis is an urgent task.

### 3. Quantum Dot-Based Nanosensors for *M. Tuberculosis* Detection and Tuberculosis Diagnosis

Most of the detection methods discussed above are in some way or another related to the detection of an optical signal, be it molecular detection methods based on PCR with fluorescent probes, lateral flow tests that use colloidal gold nanoparticles or colored latex microparticles, methods based on ELISA and ELISPOT tests, tests for CO<sub>2</sub> accumulation, or specific *M.tb* staining. Traditionally, all commercial products for MTB detection and TB diagnosis use organic fluorescent or colorimetric dyes, which have recently been increasingly replaced with fluorescent quantum dots (QDs) [42].

QDs are inorganic semiconductor nanocrystals 2–10 nm in size with a high fluorescence quantum yield due to a high molar absorption coefficient and a high efficiency of internal conversion of the absorbed photon energy into fluorescence [43]. Another benefit of QDs is their extremely long luminescence lifetime compared to fluorescent biomolecules. This allows time-resolved detection with an increased useful signal-to-noise ratio, which enhances the detection sensitivity [44,45]. The narrow emission peak and wide absorption spectrum make it possible to excite QDs of different colors with a single broad-spectrum source and perform multiplexed measurements. QDs usually have a semiconductor core (CdSe, CdS, CdTe, InP, InAs, AgInS<sub>2</sub>, CuInS<sub>2</sub>, PbSe, etc.), often coated with a shell to passivate the surface trap states and protect the core from aggressive environment and photo-oxidative degradation, as well as to meet biosafety requirements [46–48]. The typical structure of QD-based nanosensors is shown in Figure 2.

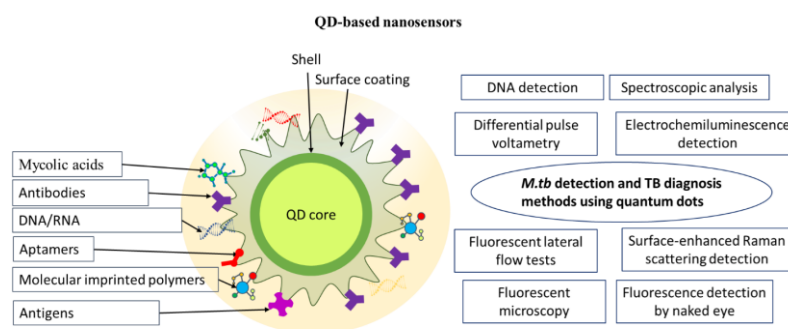


**Figure 2.** Schematics of a quantum dot-based nanosensor. Abbreviations: *M.tb*, *M. tuberculosis*; TB, tuberculosis.

An ideal QD-based fluorescence nanosensor should combine a bright fluorescent label and a highly specific recognition ligand or capture molecule [49]. This capture molecule can be a protein (e.g., an antibody or recombinant antigen), peptide, oligonucleotide, etc. [43,48,49]. After the QD-based nanosensor has bound the target biomolecule, the QD fluorescence signal can be detected and quantified [52–54]. Numerous methods for covalent and noncovalent conjugation of ligands to the QD surface (e.g., electrostatic interaction and metal ion chelation) have been developed [42,55,56]. The possibility of using multiple QDs with different emission spectra enables simultaneous detection of several biomarkers, which increases the diagnostic accuracy [57–59].

A total of 28 articles retrieved by the keywords *quantum dot*, *tuberculosis*, and *Mycobacterium tuberculosis* and 43 articles retrieved by the keywords *quantum dot* and *tuberculosis* have been found in the PubMed database. Of these publications, 37 dealt with TB diagnosis using QD-based nanosensors, 18 of them published in the past five years (including six reviews published in the past four years [7–9,60–63]). The number of these publications by year is shown in Figure 3. In total, 116 articles are cited in this review, 95 of them published in the past 10 years.

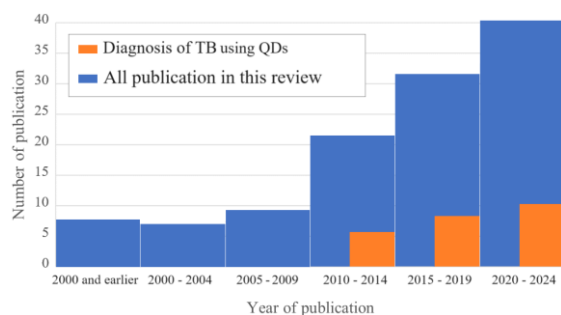


**Figure 3.** Numbers of analyzed publications by year. Abbreviations: TB, tuberculosis; QDs, quantum dots.

The methods of *M.tb* detection and TB diagnosis using QD-based nanosensors are shown in Table 2.

**Table 2.** Quantum dot-based nanosensors for *M. tuberculosis* detection and tuberculosis diagnosis.

No.	Biomaterial analyzed	Biomarker	Capture molecule	Nanosensor	Method of detection	Wavelength, nm (where relevant)	LOD	Ref.
1	Blood	TMCC1, GBP6	Oligonucleotides specific for <i>M.tb</i> mRNA biomarkers	QD655 and QD525 conjugated with the capture molecules	Toehold-mediated strand displacement with fluorescence quenching by FRET	Emission: 525 Emission: 655 Excitation: 480	GBP6: 1.6 nM TMCC1: 6.4 nM	[64]
2	Blood	IFN- $\gamma$	Anti-human IFN- $\gamma$ antibodies	CdS QDs coupled to magnetic beads conjugated with the capture molecules. Sandwich-type sensor is fabricated on a glassy carbon electrode covered with a well-ordered	Square wave anodic stripping voltammetry to quantify the metal cadmium, which indirectly	N/A	0.34 pg/mL	[65]

				gold nanoparticle monolayer, which offers a solid support to immobilize the capture molecules	reflects the amount of the analyte			
3	Serum	IFN- $\gamma$	IFN- $\gamma$ aptamer	Gold electrode covered with L-cysteine-SnTeSe QDs functionalized with the capture molecules	Electrochemical impedance spectroscopy detection of the change in the electron transfer resistance upon IFN- $\gamma$ binding	N/A	0.151 pg/mL	[66]
4	Serum	IFN- $\gamma$ , TNF- $\alpha$ , IL-2	Antibody pairs for IFN- $\gamma$ , TNF- $\alpha$ and IL-2	Sandwich immunoassay sensor consisting of luminol and carbon and CdS QDs integrated with gold nanoparticles and magnetic beads functionalized with the capture molecules, as well as the same capture molecules separately immobilized on three spatially resolved areas of a patterned indium tin oxide electrode to capture the corresponding triple latent TB biomarkers	Electrochemiluminescence detection	N/A	1.6 pg/mL	[67]
5	Sputum	DNA IS1081	Specific DNA nanobeacon	QD-based nanobeacon fluorescence probes containing QDs and black hole quenchers. After the target DNA hybridizes with the nanobeacon, the nanobeacon is cleaved into two DNA fragments, and the QDs fluoresce upon moving away from the black hole quenchers	Fluorescence detection by naked eye	Excitation: 280 Emission: 330	3.3 amol/L (2 copies/ $\mu$ L)	[68]
6	N/A	Anti-MA antibodies	MAAs	Graphene QDs covalently functionalized with MAAs as detection	Fluorescent lateral flow assay	Excitation: 360 Emission: 470	N/A	[69]

				tags for anti-MA antibodies				
7	N/A	Anti-MA antibodies	Mas	CdSe/ZnS QDs covalently functionalized with MAs as detection tags for anti-MA antibodies	Fluorescent lateral flow assay	Excitation: 390 Emission: 474	N/A	[70]
8	Pure CFP-10 solution	CFP-10	Pair of anti-CFP-10 antibodies (G2 and G3)	Glass slide coated with magnetoplasmonic core/shell nanoparticles (Fe <sub>3</sub> O <sub>4</sub> /Au) functionalized with G2. Graphene QDs functionalized with conjugate of gold-binding protein with G3. Upon binding of CFP-10 by a G2–G3 sandwich, immunoassay is formed	Dual metal-enhanced fluorescence and surface-enhanced Raman scattering detection	Excitation: 320 Emission: 436, 516	0.0511 pg/mL	[71]
9	Pure DNA	rpoB531, katG315	ssDNA specific for target DNA	QD535 and QD648 functionalized with specific ssDNA. When the target DNA is absent, the nanosensor is attached to a quencher. Binding with the target DNA leads to detachment of the nanosensor and recovery of fluorescence	Fluorescence measurement	Excitation: 380 Emission (rpoB531): 535 Emission (katG315): 648	rpoB531: 24 pM; katG315: 20 pM	[72]
10	Blood	IFN- $\gamma$ , IP-10	Aptamers specific for IFN- $\gamma$ and IP-10	Cytosine–Ag <sup>+</sup> –cytosine and thymine–Hg <sup>2+</sup> –thymine hairpin structures releasing the metal ions upon specific interaction with different biomarker–aptamer complexes. Ag <sup>+</sup> and Hg <sup>2+</sup> are bound by CdTe and carbon QDs, which are detected by fluorescence	Fluorescence measurement	-	IP-10: 0.3×10 <sup>-6</sup> pg/mL; IFN- $\gamma$ : 0.5×10 <sup>-6</sup> pg/mL	[73]
11	Sputum	<i>M.tb</i> cell	<i>M.tb</i> -binding peptide H8, anti- <i>M.tb</i> polyclonal antibodies, and anti-HSP65	QDs conjugated with H8 or anti-HSP65 antibodies and MMS conjugated with H8 or anti- <i>M.tb</i> polyclonal antibodies. Magnetic	Fluorescence microscopy	Excitation: 405 Emission: 610	103 CFU/mL	[74]

			monoclonal antibodies	separation of the QD- <i>M.tb</i> -MMS complex				
12	<i>M.tb</i> suspension and sputum	<i>M.tb</i> cell	<i>M.tb</i> -binding peptide H8	H8. Magnetic separation of the QD- <i>M.tb</i> -magnetic bead complex Magnetic beads and QDs conjugated with H8.	Fluorescence microscopy	N/A	103 CFU/mL	[75]
13	Sputum	ESAT-6	Oligonucleotides specific for ESAT-6	FRET-based sandwich biosensor containing CdTe QDs and gold nanoparticles (quencher) conjugated with the capture molecules (obtained by PCR). When the marker id bound, QD fluorescence is quenched via FRET to gold nanoparticles	Fluorescence detection	Excitation: 370 Emission: 400-680	10 fg	[76]
14	Sputum	<i>IS6110</i> DNA	ssDNA complementary to the <i>IS6110</i> gene fragment	FRET-based biosensor in which CdTe QDs conjugated with the capture molecule serves as a donor and Cu-TCPP, which is more affine for ssDNA than double-stranded DNA, serves as an acceptor. In the absence of the marker, the QD fluorescence is quenched. Interaction of the ssDNA. Hybridization of the ssDNA with the marker results in fluorescence, whose intensity depends on the marker concentration	Fluorescence detection	Excitation: 365 Emission: 586	35 pM	[77]
15	Urine	Secretory antigen Ag85B	Anti-Ag85B antibodies (GBP-50B14 and SiBP-8B3)	FRET based biosensor in which gold nanorods conjugated with GBP-50B14 serve as acceptors and silica-coated CdTe QDs conjugated with SiBP-8B3 serve as donors. When both tags bind Ag85B, FRET between the QDs and nanorods	Fluorescence detection	Excitation: 350 Emission: 630	13 pg/mL	[78]

				quenches the QD fluorescence				
16	Urine	LAM	Pair of anti-LAM recombinant monoclonal antibodies	Lateral flow test using CdSe/ZnS QDs encapsulated in polymeric bead conjugated with the capture molecules; test strip with the immobilized capture molecules	Portable fluorescence detector	Excitation: 375 Emission: 620	50 pg/mL	[79]
17	Urine	CFP-10	Pair of anti-CFP-10 antibodies	Glassy carbon electrode modified with graphene quantum dot-coated Fe <sub>3</sub> O <sub>4</sub> @Ag nanoparticles and gold nanoparticles conjugated to the capture antibody. Binding of CFP-10 to the electrode results in an immune sandwich, gold nanoparticles conjugated with the detection antibody serving as signal-amplification labels	Differential pulse voltammetry	N/A	330 pg/mL	[80]
18	Exhaled air	TB related volatile organic biomarkers	No	Suspension of CdSe or carbon QDs. The biomarker causes changes in the absorbance and fluorescence spectra.	Spectroscopic analysis	Excitation: 360–650 Emission: 300–800	N/A	[81]
19	Exhaled air	MN	Co ion	CoTCPP nanosheets with attached CdTe QDs. The QD fluorescence is quenched in the absence of MN and is recovered upon MN binding to CoTCPP causing QD release	Fluorescence detection	Excitation: 370 Emission: 658	0.59 μM	[82]
20	BALS, feces, paraffin-embedded tissues	IS6110 and IS900 DNA	Mycobacterium-specific oligonucleotides	CdSe QDs conjugated with streptavidin and species-specific probes and magnetic beads conjugated with streptavidin and genus-specific probes. Sandwich hybridization is used to bind the biomarkers and	Fluorescence detection	Excitation: 260 Emission: 655	12.5 ng	[83]

				subsequent magnet separation, to concentrate the biomarker				
21	Pure fprA	fprA	Anti-fprA antibodies	Direct and double antibody sandwich lateral flow tests with CdSe/ZnS QDs conjugated with the capture molecule	Fluorescence detection	Emission: 565	12.5 pg/mL	[84]
22	<i>M.tb</i> strains	<i>M.tb</i> DNA	ssDNA specific for <i>M.tb</i>	FRET-based sensor composed of water-stable CsPbBr <sub>3</sub> perovskite QDs conjugated to DNA probe serving as a donor and MoS <sub>2</sub> nanosheets serving as acceptor	Fluorescence detection	N/A	51.9 pM	[85]
23	Pure antigens	CFP10-ESAT6	Anti-CFP10-ESAT6 monoclonal antibody	Electrochemical immunosensor consisting of SPCE functionalized with Si nanoparticles and CdSe/ZnS QDs. The target biomarker is adsorbed on the electrode and then captured by the primary antibody, the secondary antibody being labeled with catalase, whose activity is detected electrochemically	Differential pulse voltammetry	N/A	15 pg/mL	[86]

\* Abbreviations: TMCC1, transmembrane and coiled-coil domain family 1; GBP6, guanylate binding protein family member 6; QD, quantum dot; IFN- $\gamma$ , interferon gamma; TNF- $\alpha$ , tumor necrosis factor alpha; IL-2, interleukin-2; MAs, mycolic acids; CFP-10, culture filtrate protein 10; ssDNA, single-strand DNA; IP-10, IFN- $\gamma$ -induced protein 10; MMS, magnetic microsphere; HSP65, heat shock protein 65; ESAT-6, early secretory antigenic target 6; FRET, Förster resonance energy transfer; Cu-TCPP, two-dimensional metal-organic framework; LAM, lipoarabinomannan; MN, methyl nicotinate; CoTCPP, cobalt-metalized tetrakis (4-carboxyphenyl) porphyrin; BALS, bronchoalveolar lavage specimens; fprA, flavoprotein reductase; SPCE, screen-printed carbon electrode; DPV, differential pulse voltammetry.

Not all of the biomarkers described above are completely specific, because their occurrence may be related to concomitant diseases, body conditions, etc. Currently, there is no biomarker or combination of biomarkers that allows diagnosing active forms of TB with an accuracy close to 100%. Thus, the search for a combination of biomarkers with a high specificity is an urgent task. New potential *M.tb* biomarkers that can be detected by new QD-based fluorescent nanosensors are listed in Table 3.

**Table 3.** Potential *M. tuberculosis* biomarkers.

225  
226  
227  
228  
229  
230  
231  
232  
233  
234  
235  
236  
237  
238  
239  
240

Biomarker	Already detected with QD-based nanosensors	Comment	Ref.
<b>Host RNA transcript/DNA signatures</b>			
GBP2, GBP5, GBP6, TMCC1	+	Oligonucleotides (RNA, DNA)	[64,87]
PRDM1	-	PR domain zinc finger protein 1 gene	[87]
ARG1	-	Arginase 1 gene (encoding the arginase enzyme)	[87]
IS6110	+	IS6110 gene	[77]
IS1081	-	IS1081 gene	[88]
rpoB531	+	rpoB531 gene	[72]
katG315	+	katG315 gene	[72]
<b>Acids and their derivatives</b>			
MN	+	Menthyl nicotinate	[81]
MAs	+	Mycolic acids	[69,70]
<b>Enzymes</b>			
MNAzymes	+	Multicomponent nucleic acid enzyme	[68]
ADA	-	Adenosine deaminase (enzyme of purine metabolism)	[89]
KatGs	-	Catalase-peroxidase enzymes (responsible for the activation of the antituberculosis drug isoniazid)	[90]
<b>Cytokines</b>			
IL-1ra		Interleukin-1 receptor antagonist	[91]
IL-2	+	Interleukin-2	[91,92]
IL-10	+	Interleukin-10	[91,93]
IL-13		Interleukin-13	[91]
INF- $\gamma$	+	Interferon gamma	[65,92,93]
TNF- $\alpha$	+	Tumor necrosis factor alpha	[92]
INF- $\gamma$ IP-10	+	Interferon-gamma-inducible protein 10	[25]
MIP-1 $\beta$	-	Macrophage inflammatory protein	[91]
<b>Specific surface proteins</b>			
CFP-10	+	10-kDa culture-filtered protein	[86,94,95]
Mtb Rv1468c (PE_PGRS29)	-	<i>M.tb</i> surface protein	[96]
Rv1509	-	<i>M.tb</i> -specific protein	[97]
ESAT-6	-	6-kDa early secreted antigenic target	[94,98–100]
MPT-64	-	<i>M.tb</i> protein 64	[101]
Ag85B	+	Secreted protein antigen 85 complex B	[78,102]
PPE-68	-	Proline-proline-glutamic acid	[103,104]
Rv2536	-	Potential membrane protein	[105]
Rv2341		Probable conserved lipoprotein LppQ	[106]
<b>Mycobacterial antigens</b>			
14-kDa antigen	-	14-kDa protein antigen	[107]
16-kDa antigen	-	<i>M.tb</i> -specific antigens	[108]
19-kDa antigen	-	19-kDa lipoprotein	[107]
30-kDa antigen	-	Immunodominant phosphate-binding protein	[109]
38-kDa antigen	-	Immunodominant lipoprotein antigen	[110]
55-kDa antigen	-	<i>M.tb</i> -specific antigens	[111]
LAM	-	A glycolipid and a virulence factor associated with <i>M.tb</i>	[112]
A60	-	Tuberculosis antigen	[113]
Mtb81	-	Recombinant protein	[114]



ESAT-6

+

*M.tb*-specific antigens

[86,115]

Host transcript RNA/DNA signatures is a group of biomarkers associated with the host gene expression in response to *M.tb* infection. For some markers listed in Table 3, there are suitable QD-based nanosensors presented in Table 2 (GBP2 [64,87], GBP5 [64,87], GBP6 [64,87], IS6110 gene [77], rpoB531 gene [72], and katG315gene [72]). Regarding PRDM1, it is also associated with lymphoma [116]. To date, there is no QD-based nanosensor for arginase 1 detection. The group of acids and their derivatives consists of two important TB biomarkers: MN [81] and MAs [69,70]. For both markers, sets of QDs and conjugates that can be used for TB diagnosis are shown in Table 2. Three most common enzymes can be used for TB diagnosis: MNAzymes, ADA, and KatG. To date, QDs functionalized with MNAzymes [68] have been proposed as TB diagnostic agents. Regarding KatGs, there are methods for detecting the encoding genes, but there are no biosensors for detecting the enzymes themselves. No nanosensors for ADA detection have been reported to date.

The groups of specific surface protein and mycobacterial antigen biomarkers can be pooled because both include specific proteins and other antigens associated with *M.tb*. At the moment, three main protein antigens from this group have been studied for TB diagnosis using nanosensors: CFP-10, ESAT-6, and Ag85B [71,78,80,86].

#### 4. Summary and Outlook

TB remains a major global health problem, with millions of new cases and significant mortality every year. Early and accurate diagnosis is crucial for effective treatment and control of this disease. Traditional methods of TB diagnosis, such as PCR tests, immunofluorescence and immunochemical analyses, flow cytometry, cell culture tests, and microscopic analysis can be improved by the use of optical tags based on fluorescent QDs. Some alternative nanomaterials, such as other nanoparticles [114–116], graphene [88], and graphene-like 2D-materials (trans-graphenes) [113,117–122], can also be used for the development of nanosensors solving similar tasks and based on the same physical principles. QDs have already established themselves as promising constituent elements of biosensors providing increased sensitivity and specificity of detection than routinely used assays and allowing the development of multiplexed assays for early, more detailed detection of *M.tb* and diagnosis of TB. Despite the undoubtedly high potential, several challenges need to be addressed for enabling widespread use of QD-based nanosensors for TB diagnosis, such as the search for new suitable conjugates and available highly specific biomarkers, standardization and validation of diagnostic protocols, and advanced cost- and time-reducing solutions. However, the data reviewed here show that the unique properties of QDs make the QD-based nanosensors promising candidates for biosensing applications, including *in vitro* *M.tb* diagnosis. The use of QDs makes it possible to increase the sensitivity and speed of analysis, which is important for point-of-care diagnosis of TB and wider coverage of diagnostic procedures. The possibility of excitation of QD fluorescence in a wide range of wavelengths and a long fluorescence lifetime allow reducing the requirements for fluorescence detectors and, hence, the cost of their manufacture, as well as designing more compact devices for reading the fluorescent signal. This could ensure their wider use of these tools in diagnostic practice, thus decreasing the morbidity and mortality from TB.

**Author Contributions:** Conceptualization, Yu.V.K. and I.R.N.; writing—original draft preparation, V.V.N and P.M.S.; writing—review and editing, T.B.L, A.S.A., E.B.; data validation and general revision, P.M.S.; supervision, I.R.N. and Yu.V.K.; funding acquisition, Yu.V.K. and I.R.N. All authors have read and agreed to the published version of the manuscript.

**Funding:** The part of the study related to design of the quantum sensors was funded by the Russian Science Foundation (RSF) grant number 21-79-30048. The part of the study related to the quantum sensors biomedical applications was funded by the RSF grant number 23-75-30016.

**Institutional Review Board Statement:** Not applicable.

**Informed Consent Statement:** Not applicable.

**Data Availability Statement:** Not applicable.

**Acknowledgments:** We thank Vladimir Ushakov for proofreading the manuscript and Maria Ya. Stoyanova for assistance in filling in the data on the standard methods for tuberculosis diagnosis.

**Conflicts of Interest:** The authors declare no conflicts of interest. The funders had no role in the design of the study; in the collection, analyses, or interpretation of data; in the writing of the manuscript; or in the decision to publish the results. The company Life Improvement by Future Technologies (LIFT) Center had no role in the design of the study; in the collection, analyses, or interpretation of data; in the writing of the manuscript; or in the decision to publish the results.

## References

1. The Global Health Observatory: SDG Target 3.3 Communicable diseases. Available online: [https://Www.Who.Int/Data/Gho/Data/Themes/Topics/Sdg-Target-3\\_3-Communicable-Diseases](https://Www.Who.Int/Data/Gho/Data/Themes/Topics/Sdg-Target-3_3-Communicable-Diseases).
2. Tuberculosis in Women, World Health Organization, Fact Sheet October 2016. Available online: <http://Www.Who.Int/Tb/Areas-of-Work/Population-Groups/Gender/En/>.
3. Chakaya, J.; Khan, M.; Ntoumi, F.; Aklillu, E.; Fatima, R.; Mwaba, P.; Kapata, N.; Mfinanga, S.; Hasnain, S.E.; Katoto, P.D.M.C.; et al. Global Tuberculosis Report 2020 – Reflections on the global TB burden, treatment and prevention efforts. *Int. J. Infect. Dis.* **2021**, *113*, S7–S12, doi:10.1016/j.ijid.2021.02.107.
4. Maddineni, M.; Panda, M. Pulmonary tuberculosis in a young pregnant female: Challenges in diagnosis and management. *Infect. Dis. Obst. Gynecol.* **2008**, *2008*, 1–5, doi:10.1155/2008/628985.
5. Liu, Q.; Yang, X.; Wen, J.; Tang, D.; Qi, M.; He, J. Host factors associated with false negative results in an interferon -  $\gamma$  release assay in adults with active tuberculosis. *Heliyon* **2023**, *9*, e22900, doi:10.1016/j.heliyon.2023.e22900.
6. World Health Organization. *Guidelines on the Management of Latent Tuberculosis Infection*. World Health Organization, 2015.
7. Yang, X.; Fan, S.; Ma, Y.; Chen, H.; Xu, J.-F.; Pi, J.; Wang, W.; Chen, G. Current progress of functional nanobiosensors for potential tuberculosis diagnosis: The novel way for TB control? *Front. Bioeng. Biotechnol.* **2022**, *10*, 1036678, doi:10.3389/fbioe.2022.1036678.
8. Mukherjee, S.; Perveen, S.; Negi, A.; Sharma, R. Evolution of tuberculosis diagnostics: From molecular strategies to nanodiagnosics. *Tuberculosis* **2023**, *140*, 102340, doi:10.1016/j.tube.2023.102340.
9. Gupta, A.K.; Singh, A.; Singh, S. Diagnosis of tuberculosis: Nanodiagnosics approaches. In *NanoBioMedicine*; Saxena, S.K., Khurana, S.M.P., Eds.; Springer: Singapore, 2020; pp. 261–283 ISBN 978-981-329-897-2.
10. Jin, T.; Fei, B.; Zhang, Y.; He, X. The diagnostic value of polymerase chain reaction for *Mycobacterium tuberculosis* to distinguish intestinal tuberculosis from Crohn’s disease: A meta-analysis. *Saudi J Gastroenterol.* **2017**, *23*, 3, doi:10.4103/1319-3767.199135.
11. Steingart, K.R.; Schiller, I.; Horne, D.J.; Pai, M.; Boehme, C.C.; Dendukuri, N. Xpert MTB/RIF assay for pulmonary tuberculosis and rifampicin resistance in adults. In: *Cochrane Database of Systematic Reviews* **2014**, doi:10.1002/14651858.CD009593.pub3.
12. Ssengooba, W.; Katamba, A.; Sserubiri, J.; Semugenze, D.; Nyombi, A.; Byaruhanga, R.; Turyahabwe, S.; Joloba, M.L. Performance evaluation of Truenat MTB and Truenat MTB-RIF DX assays in comparison to Gene XPERT MTB/RIF Ultra for the diagnosis of pulmonary tuberculosis in Uganda. *BMC Infect. Dis.* **2024**, *24*, 190, doi:10.1186/s12879-024-09063-z.
13. Bjerrum, S.; Schiller, I.; Dendukuri, N.; Kohli, M.; Nathavitharana, R.R.; Zwerling, A.A.; Denking, C.M.; Steingart, K.R.; Shah, M. Lateral flow urine lipoarabinomannan assay for detecting active tuberculosis in people living with HIV. In: *Cochrane Database of Systematic Reviews* **2019**, 2019, doi:10.1002/14651858.CD011420.pub3.

14. Manga, S.; Perales, R.; Reaño, M.; D'Ambrosio, L.; Migliori, G.B.; Amicosante, M. Performance of a lateral flow immunochromatography test for the rapid diagnosis of active tuberculosis in a large multicentre study in areas with different clinical settings and tuberculosis exposure levels. *J. Thorac. Dis.* **2016**, *8*, 3307–3313, doi:10.21037/jtd.2016.11.51. 332–334
15. Chen, H.; Nakagawa, A.; Takamori, M.; Abe, S.; Ueno, D.; Horita, N.; Kato, S.; Seki, N. Diagnostic accuracy of the interferon-gamma release assay in acquired immunodeficiency syndrome patients with suspected tuberculosis infection: A meta-analysis. *Infection* **2022**, *50*, 597–606, doi:10.1007/s15010-022-01789-9. 335–337
16. Tortoli, E.; Mandler, F.; Tronci, M.; Penati, V.; Sbaraglia, G.; Costa, D.; Montini, G.; Predominato, M.; Riva, R.; Passerini Tosi, C.; et al. Multicenter evaluation of mycobacteria growth indicator tube (MGIT) compared with the BACTEC radiometric method, BBL biphasic growth medium and Löwenstein–Jensen medium. *Clin. Microbiol. Infect.* **1997**, *3*, 468–473, doi:10.1111/j.1469-0691.1997.tb00284.x. 338–341
17. Cruciani, M.; Scarparo, C.; Malena, M.; Bosco, O.; Serpelloni, G.; Mengoli, C. Meta-analysis of BACTEC MGIT 960 and BACTEC 460 TB, with or without solid media, for detection of mycobacteria. *J. Clin. Microbiol.* **2004**, *42*, 2321–2325, doi:10.1128/JCM.42.5.2321-2325.2004. 342–344
18. Martinez, M.R.; Sardiñas, M.; Garcia, G.; Mederos, L.M.; Díaz, R. Evaluation of BacT/ALERT 3D system for mycobacteria isolates. *J. Tuberc. Res.* **2014**, *2*, 59–64, doi:10.4236/jtr.2014.22007. 345–346
19. Rose, D.N.; Schechter, C.B.; Adler, J.J. Interpretation of the tuberculin skin test. *J. Gen. Intern. Med.* **1995**, *10*, 635–642, doi:10.1007/BF02602749. 347–348
20. Abdelaziz, M.M.; Bakr, W.M.K.; Hussien, S.M.; Amine, A.E.K. Diagnosis of pulmonary tuberculosis using Ziehl–Neelsen stain or cold staining techniques? *J. Egypt. Pub. Health Assoc.* **2016**, *91*, 39–43, doi:10.1097/01.EPX.0000481358.12903.af. 349–350
21. Cattamanchi, A.; Davis, J.L.; Worodria, W.; den Boon, S.; Yoo, S.; Matovu, J.; Kiidha, J.; Nankya, F.; Kyeyune, R.; Byanyima, P.; et al. Sensitivity and specificity of fluorescence microscopy for diagnosing pulmonary tuberculosis in a high HIV prevalence setting. *Int. J. Tuberc. Lung Dis.* **2009**, *13*, 1130–1136. 351–353
22. Pinto, L.M.; Pai, M.; Dheda, K.; Schwartzman, K.; Menzies, D.; Steingart, K.R. Scoring systems using chest radiographic features for the diagnosis of pulmonary tuberculosis in adults: A systematic review. *Eur. Respir. J.* **2013**, *42*, 480–494, doi:10.1183/09031936.00107412. 354–356
23. Wang, Y.; Xu, Q.; Xu, B.; Lin, Y.; Yang, X.; Tong, J.; Huang, C. Clinical performance of nucleotide MALDI-TOF-MS in the rapid diagnosis of pulmonary tuberculosis and drug resistance. *Tuberculosis* **2023**, *143*, 102411, doi:10.1016/j.tube.2023.102411. 357–358
24. Metcalfe, J.; Bacchetti, P.; Esmail, A.; Reckers, A.; Aguilar, D.; Wen, A.; Huo, S.; Muyindike, W.R.; Hahn, J.A.; Dheda, K.; et al. Diagnostic accuracy of a liquid chromatography-tandem mass spectrometry assay in small hair samples for rifampin-resistant tuberculosis drug concentrations in a routine care setting. *BMC Infect. Dis.* **2021**, *21*, 99, doi:10.1186/s12879-020-05738-5. 359–361
25. Nsubuga, G.; Kennedy, S.; Rani, Y.; Hafiz, Z.; Kim, S.; Ruhwald, M.; Alland, D.; Ellner, J.; Joloba, M.; Dorman, S.E.; et al. Diagnostic accuracy of the NOVA tuberculosis total antibody rapid test for detection of pulmonary tuberculosis and infection with *Mycobacterium tuberculosis*. *J. Clin. Tuberc. Other Mycobacter. Dis.* **2023**, *31*, 100362, doi:10.1016/j.jctube.2023.100362. 362–364
26. Sharma, G.; Tewari, R.; Dhatwalia, S.K.; Yadav, R.; Behera, D.; Sethi, S. A loop-mediated isothermal amplification assay for the diagnosis of pulmonary tuberculosis. *Lett. Appl. Microbiol.* **2019**, *68*, 219–225, doi:10.1111/lam.13115. 365–366
27. *The Use of Loop-Mediated Isothermal Amplification (TB-LAMP) for the Diagnosis of Pulmonary Tuberculosis: Policy Guidance*; WHO Guidelines Approved by the Guidelines Review Committee; World Health Organization: Geneva, 2016; ISBN 978-92-4-151118-6. 367–369
28. Horne, D.J.; Kohli, M.; Zifodya, J.S.; Schiller, I.; Dendukuri, N.; Tollefson, D.; Schumacher, S.G.; Ochodo, E.A.; Pai, M.; Steingart, K.R. Xpert MTB/RIF and Xpert MTB/RIF Ultra for pulmonary tuberculosis and rifampicin resistance in adults. In: *Cochrane Database of Systematic Reviews* **2019**, doi:10.1002/14651858.CD009593.pub4. 370–372

29. Aainouss, A.; Momen, Gh.; Belghiti, A.; Bennani, K.; Lamaammal, A.; Chetioui, F.; Messaoudi, M.; Blaghen, M.; Mouslim, J.; Khyatti, M.; et al. Performance of GeneXpert MTB/RIF in the diagnosis of extrapulmonary tuberculosis in Morocco. *Rus. J. Infect. Immun.* **2021**, *12*, 78–84, doi:10.15789/2220-7619-POG-1695.
30. Ngangue, Y.R.; Mbuli, C.; Neh, A.; Nshom, E.; Koudjou, A.; Palmer, D.; Ndi, N.N.; Qin, Z.Z.; Creswell, J.; Mbassa, V.; et al. Diagnostic accuracy of the Truenat MTB Plus assay and comparison with the Xpert MTB/RIF assay to detect tuberculosis among hospital outpatients in Cameroon. *J. Clin. Microbiol.* **2022**, *60*, e00155-22, doi:10.1128/jcm.00155-22.
31. Sevastyanova, E.V.; Smirnova, T.G.; Larionova, E.E.; Chernousova, L.N. Detection of mycobacteria by culture inoculation. Liquid media and automated systems. *Bulle. TsNIIT* **2020**, 88–95, doi:10.7868/S258766782004010X.
32. Lee, H.S.; Park, K.U.; Park, J.O.; Chang, H.E.; Song, J.; Choe, G. Rapid, sensitive, and specific detection of *Mycobacterium tuberculosis* complex by real-time PCR on paraffin-embedded human tissues. *J. Mol. Diagn.* **2011**, *13*, 390–394, doi:10.1016/j.jmoldx.2011.02.004.
33. Itani, L.Y.; Cherry, M.A.; Araj, G.F. Efficacy of BACTEC TB in the rapid confirmatory diagnosis of mycobacterial infections: A Lebanese tertiary care center experience. *J. Med. Liban.* **2005**, *53*, 208–212.
34. Campelo, T.A.; Cardoso De Sousa, P.R.; Nogueira, L.D.L.; Frota, C.C.; Zuquim Antas, P.R. Revisiting the methods for detecting mycobacterium tuberculosis: What has the new millennium brought thus far? *Access Microbio.* **2021**, *3*, doi:10.1099/acmi.0.000245.
35. Szewczyk, R.; Kowalski, K.; Janiszewska-Drobinska, B.; Druszczyńska, M. Rapid method for *Mycobacterium tuberculosis* identification using electrospray ionization tandem mass spectrometry analysis of mycolic acids. *Diagn. Microbiol. Infect. Dis.* **2013**, *76*, 298–305, doi:10.1016/j.diagmicrobio.2013.03.025.
36. El Khéchine, A.; Couderc, C.; Flaudrops, C.; Raoult, D.; Drancourt, M. Matrix-assisted laser desorption/ionization time-of-flight mass spectrometry identification of mycobacteria in routine clinical practice. *PLoS ONE* **2011**, *6*, e24720, doi:10.1371/journal.pone.0024720.
37. Bacanelli, G.; Araujo, F.R.; Verbisck, N.V. Improved MALDI-TOF MS identification of *Mycobacterium tuberculosis* by use of an enhanced cell disruption protocol. *Microorganisms* **2023**, *11*, 1692, doi:10.3390/microorganisms11071692.
38. Thomas, S.N.; French, D.; Jannetto, P.J.; Rappold, B.A.; Clarke, W.A. Liquid chromatography–tandem mass spectrometry for clinical diagnostics. *Nat Rev. Meth. Primers* **2022**, *2*, 96, doi:10.1038/s43586-022-00175-x.
39. Malo, A.; Kellermann, T.; Ignatius, E.H.; Dooley, K.E.; Dawson, R.; Joubert, A.; Norman, J.; Castel, S.; Wiesner, L. A Validated liquid chromatography tandem mass spectrometry assay for the analysis of pretomanid in plasma samples from pulmonary tuberculosis patients. *J. Pharmac. Biomed. Anal.* **2021**, *195*, 113885, doi:10.1016/j.jpba.2020.113885.
40. Chen, H.; Li, S.; Zhao, W.; Deng, J.; Yan, Z.; Zhang, T.; Wen, S.A.; Guo, H.; Li, L.; Yuan, J.; et al. A peptidomic approach to identify novel antigen biomarkers for the diagnosis of tuberculosis. *Infect. Dis. Rep.* **2022**, *15*, 4617–4626, doi:10.2147/IDR.S373652.
41. Chen, X.; Song, B.; Jiang, H.; Yu, K.; Zhong, D. A liquid chromatography/tandem mass spectrometry method for the simultaneous quantification of isoniazid and ethambutol in human plasma. *Rapid Commun. Mass Spectrom.* **2005**, *19*, 2591–2596, doi:10.1002/rcm.2100.
42. He, X.; Ma, N. An overview of recent advances in quantum dots for biomedical applications. *Colloids Surf. B Biointerfaces* **2014**, *124*, 118–131, doi:10.1016/j.colsurfb.2014.06.002.
43. Medintz, I.L.; Uyeda, H.T.; Goldman, E.R.; Mattoussi, H. Quantum dot bioconjugates for imaging, labelling and sensing. *Nat. Mat.* **2005**, *4*, 435–446, doi:10.1038/nmat1390.
44. Brkić, S. Applicability of quantum dots in biomedical science. In *Ionizing Radiation Effects and Applications*; Djezzar, B., Ed.; InTech, 2018. ISBN 978-953-51-3953-9.
45. Samokhvalov, P.S.; Karaulov, A.V.; Nabiev, I.R. Control of the photoluminescence lifetime of quantum dots by engineering their shell structure. *Opt. Spektrosk.* **2023**, *131*, 1262–1267 [in Russian], doi:10.61011/OS.2023.09.56614.5586-23.

46. Bilan, R.; Nabiev, I.; Sukhanova, A. quantum dot - based nanotools for bioimaging, diagnostics, and drug delivery. *ChemBioChem* **2016**, *17*, 2103–2114, doi:10.1002/cbic.201600357. 414  
415
47. Sukhanova, A.; Ramos-Gomes, F.; Chames, P.; Sokolov, P.; Baty, D.; Alves, F.; Nabiev, I. Multiphoton deep-tissue imaging of micrometastases and disseminated cancer cells using conjugates of quantum dots and single-domain antibodies. In *Multiplexed Imaging*; Zamir, E., Ed.; Methods in Molecular Biology; Springer: New York, NY, 2021; Volume 2350, pp. 105–123 ISBN 978-1-07-161592-8. 416  
417  
418  
419
48. Sokolov, P.; Samokhvalov, P.; Sukhanova, A.; Nabiev, I. Biosensors based on inorganic composite fluorescent hydrogels. *Nanomaterials* **2023**, *13*, 1748, doi:10.3390/nano13111748. 420  
421
49. Hafian, H.; Sukhanova, A.; Turini, M.; Chames, P.; Baty, D.; Pluot, M.; Cohen, J.H.M.; Nabiev, I.; Millot, J.-M. Multiphoton imaging of tumor biomarkers with conjugates of single-domain antibodies and quantum dots. *Nanomedicine: NBM* **2014**, *10*, 1701–1709, doi:10.1016/j.nano.2014.05.014. 422  
423  
424
50. Bilan, R.; Fleury, F.; Nabiev, I.; Sukhanova, A. Quantum dot surface chemistry and functionalization for cell targeting and imaging. *Bioconjugate Chem.* **2015**, *26*, 609–624, doi:10.1021/acs.bioconjchem.5b00069. 425  
426
51. Sukhanova, A.; Even-Desrumeaux, K.; Kisserli, A.; Tabary, T.; Reveil, B.; Millot, J.-M.; Chames, P.; Baty, D.; Artemyev, M.; Oleinikov, V.; et al. Oriented conjugates of single-domain antibodies and quantum dots: Toward a new generation of ultrasmall diagnostic nanoproboscopes. *Nanomedicine: NBM* **2012**, *8*, 516–525, doi:10.1016/j.nano.2011.07.007. 427  
428  
429
52. Lee, J.S.; Youn, Y.H.; Kwon, I.K.; Ko, N.R. Recent advances in quantum dots for biomedical applications. *J. Pharmac. Invest.* **2018**, *48*, 209–214, doi:10.1007/s40005-018-0387-3. 430  
431
53. Han, X.; Xu, K.; Taratula, O.; Farsad, K. Applications of nanoparticles in biomedical imaging. *Nanoscale* **2019**, *11*, 799–819, doi:10.1039/C8NR07769J. 432  
433
54. Zhang, Y.; Cai, N.; Chan, V. Recent advances in silicon quantum dot-based fluorescent biosensors. *Biosensors* **2023**, *13*, 311, doi:10.3390/bios13030311. 434  
435
55. Brazhnik, K.; Nabiev, I.; Sukhanova, A. Oriented conjugation of single-domain antibodies and quantum dots. In *Quantum Dots: Applications in Biology*; Fontes, A., Santos, B.S., Eds.; Methods in Molecular Biology; Springer: New York, NY, 2014; Volume 1199, pp. 129–140 ISBN 978-1-4939-1279-7. 436  
437  
438
56. Brazhnik, K.; Nabiev, I.; Sukhanova, A. Advanced procedure for oriented conjugation of full-size antibodies with quantum dots. In *Quantum Dots: Applications in Biology*; Fontes, A., Santos, B.S., Eds.; Methods in Molecular Biology; Springer: New York, NY, 2014; Volume 1199, pp. 55–66 ISBN 978-1-4939-1279-7. 439  
440  
441
57. Biju, V. Chemical modifications and bioconjugate reactions of nanomaterials for sensing, imaging, drug delivery and therapy. *Chem. Soc. Rev.* **2014**, *43*, 744–764, doi:10.1039/C3CS60273G. 442  
443
58. Bilan, R.S.; Krivenkov, V.A.; Berestovoy, M.A.; Efimov, A.E.; Agapov, I.I.; Samokhvalov, P.S.; Nabiev, I.; Sukhanova, A. Engineering of optically encoded microbeads with FRET-free spatially separated quantum - dot layers for multiplexed assays. *ChemPhysChem* **2017**, *18*, 970–979, doi:10.1002/cphc.201601274. 444  
445  
446
59. Rousserie, G.; Sukhanova, A.; Even-Desrumeaux, K.; Fleury, F.; Chames, P.; Baty, D.; Oleinikov, V.; Pluot, M.; Cohen, J.H.M.; Nabiev, I. Semiconductor quantum dots for multiplexed bio-detection on solid-state microarrays. *Crit. Rev. Oncol. Hematol.* **2010**, *74*, 1–15, doi:10.1016/j.critrevonc.2009.04.006. 447  
448  
449
60. Sarkar, L.H.; Kumari, S. Nanocarriers for *Mycobacterium tuberculosis*. *J. Sci. Res.* **2021**, *65*, 33–37, doi:10.37398/JSR.2021.650807. 450
61. El-Shabasy, R.M.; Zahran, M.; Ibrahim, A.H.; Maghraby, Y.R.; Nayel, M. Advances in the fabrication of potential nanomaterials for diagnosis and effective treatment of tuberculosis. *Mater. Adv.* **2024**, *5*, 1772–1782, doi:10.1039/D3MA00720K. 451  
452
62. Ahmad, F.; Pandey, N.; Singh, K.; Ahmad, S.; Khubaib, M.; Sharma, R. Recent advances in nanocarrier based therapeutic and diagnostic approaches in tuberculosis. *Prec. Nanomed.* **2023**, *6*, doi:10.33218/001c.90699. 453  
454

63. Pati, R.; Sahu, R.; Panda, J.; Sonawane, A. Encapsulation of zinc-rifampicin complex into transferrin-conjugated silver quantum-dots improves its antimycobacterial activity and stability and facilitates drug delivery into macrophages. *Sci. Rep.* **2016**, *6*, 24184, doi:10.1038/srep24184. 455-457
64. Gliddon, H.D.; Howes, P.D.; Kaforou, M.; Levin, M.; Stevens, M.M. A nucleic acid strand displacement system for the multiplexed detection of tuberculosis-specific mRNA using quantum dots. *Nanoscale* **2016**, *8*, 10087–10095, doi:10.1039/C6NR00484A. 458-460
65. Huang, H.; Li, J.; Shi, S.; Yan, Y.; Zhang, M.; Wang, P.; Zeng, G.; Jiang, Z. Detection of interferon-gamma for latent tuberculosis diagnosis using an immunosensor based on CdS quantum dots coupled to magnetic beads as labels. *Int. J. Electrochem. Sci.* **2015**, *10*, 2580–2593, doi:10.1016/S1452-3981(23)04869-1. 461-463
66. Januarie, K.C.; Oranzie, M.; Feleni, U.; Iwuoha, E. Quantum dot amplified impedimetric aptasensor for interferon-gamma. *Electrochim. Acta* **2023**, *463*, 142825, doi:10.1016/j.electacta.2023.142825. 464-465
67. Zhou, B.; Zhu, M.; Hao, Y.; Yang, P. Potential-resolved electrochemiluminescence for simultaneous determination of triple latent tuberculosis infection markers. *ACS Appl. Mater. Interfaces* **2017**, *9*, 30536–30542, doi:10.1021/acsami.7b10343. 466-467
68. Hu, O.; Li, Z.; Wu, J.; Tan, Y.; Chen, Z.; Tong, Y. A multicomponent nucleic acid enzyme-cleavable quantum dot nanobeacon for highly sensitive diagnosis of tuberculosis with the naked eye. *ACS Sens.* **2023**, *8*, 254–262, doi:10.1021/acssensors.2c02114. 468-469
69. Kabwe, K.P.; Nsibande, S.A.; Pilcher, L.A.; Forbes, P.B.C. Development of a mycolic acid - graphene quantum dot probe as a potential tuberculosis biosensor. *Luminescence* **2022**, *37*, 1881–1890, doi:10.1002/bio.4368. 470-471
70. Kabwe, K.P.; Nsibande, S.A.; Lemmer, Y.; Pilcher, L.A.; Forbes, P.B.C. Synthesis and characterisation of quantum dots coupled to mycolic acids as a water - soluble fluorescent probe for potential lateral flow detection of antibodies and diagnosis of tuberculosis. *Luminescence* **2022**, *37*, 278–289, doi:10.1002/bio.4170. 472-474
71. Zou, F.; Zhou, H.; Tan, T.V.; Kim, J.; Koh, K.; Lee, J. Dual-mode SERS-fluorescence immunoassay using graphene quantum dot labeling on one-dimensional aligned magnetoplasmonic nanoparticles. *ACS Appl. Mater. Interfaces* **2015**, *7*, 12168–12175, doi:10.1021/acsami.5b02523. 475-477
72. Hu, O.; Li, Z.; He, Q.; Tong, Y.; Tan, Y.; Chen, Z. Fluorescence biosensor for one-step simultaneous detection of *Mycobacterium tuberculosis* multidrug-resistant genes using nanoCoTPyP and double quantum dots. *Anal. Chem.* **2022**, *94*, 7918–7927, doi:10.1021/acs.analchem.2c00723. 478-480
73. Shi, T.; Jiang, P.; Peng, W.; Meng, Y.; Ying, B.; Chen, P. Nucleic acid and nanomaterial synergistic amplification enables dual targets of ultrasensitive fluorescence quantification to improve the efficacy of clinical tuberculosis diagnosis. *ACS Appl. Mater. Interfaces* **2024**, *16*, 14510–14519, doi:10.1021/acsami.3c18596. 481-483
74. Yang, H.; Qin, L.; Wang, Y.; Zhang, B.; Liu, Z.; Ma, H.; Lu, J.; Huang, X.; Shi, D.; Hu, Z. Detection of *Mycobacterium tuberculosis* based on H<sub>37</sub>R<sub>v</sub> binding peptides using surface functionalized magnetic microspheres coupled with quantum dots—A Nano detection method for *Mycobacterium tuberculosis*. *Int. J. Nanomed.* **2014**, *77*, doi:10.2147/IJN.S71700. 484-486
75. Ma, H.; Hu, Z.; Wang, Y.; Qing, L.; Chen, H.; Lu, J.; Yang, H. [Methodology research and preliminary assessment of *Mycobacterium tuberculosis* detection by immunomagnetic beads combined with functionalized fluorescent quantum dots]. *Zhonghua Jie He He Hu Xi Za Zhi (Chin. J. Tuberc. Resp. Dis.)* **2013**, *36*, 100–105 [in Chinese]. 487-489
76. Shojaei, T.R.; Mohd Salleh, M.A.; Tabatabaei, M.; Ekrami, A.; Motallebi, R.; Rahmani-Cherati, T.; Hajalilou, A.; Jorfi, R. Development of sandwich-form biosensor to detect mycobacterium tuberculosis complex in clinical sputum specimens. *Braz. J. Infect. Dis.* **2014**, *18*, 600–608, doi:10.1016/j.bjid.2014.05.015. 490-492
77. Liang, L.; Chen, M.; Tong, Y.; Tan, W.; Chen, Z. Detection of *Mycobacterium tuberculosis* IS6110 gene fragment by fluorescent biosensor based on FRET between two-dimensional metal-organic framework and quantum dots-labeled DNA probe. *Anal. Chim. Acta* **2021**, *1186*, 339090, doi:10.1016/j.aca.2021.339090. 493-495

78. Kim, E.J.; Kim, E.B.; Lee, S.W.; Cheon, S.A.; Kim, H.-J.; Lee, J.; Lee, M.-K.; Ko, S.; Park, T.J. An easy and sensitive sandwich assay for detection of *Mycobacterium tuberculosis* Ag85B antigen using quantum dots and gold nanorods. *Biosens. Bioelectron.* **2017**, *87*, 150–156, doi:10.1016/j.bios.2016.08.034.
79. Huang, Z.; Huang, H.; Hu, J.; Xia, L.; Liu, X.; Qu, R.; Huang, X.; Yang, Y.; Wu, K.; Ma, R.; et al. A novel quantitative urine LAM Antigen strip for point-of-care tuberculosis diagnosis in non-HIV adults. *J. Infect.* **2024**, *88*, 194–198, doi:10.1016/j.jinf.2023.11.014.
80. Tufa, L.T.; Oh, S.; Tran, V.T.; Kim, J.; Jeong, K.-J.; Park, T.J.; Kim, H.-J.; Lee, J. Electrochemical immunosensor using nanotriplex of graphene quantum dots, Fe<sub>3</sub>O<sub>4</sub>, and Ag nanoparticles for tuberculosis. *Electrochim. Acta* **2018**, *290*, 369–377, doi:10.1016/j.electacta.2018.09.108.
81. Bhattacharyya, D.; Sarswat, P.K.; Free, M.L. Quantum dots and carbon dots based fluorescent sensors for TB biomarkers detection. *Vacuum* **2017**, *146*, 606–613, doi:10.1016/j.vacuum.2017.02.003.
82. He, Q.; Cai, S.; Wu, J.; Hu, O.; Liang, L.; Chen, Z. Determination of tuberculosis-related volatile organic biomarker methyl nicotinate in vapor using fluorescent assay based on quantum dots and cobalt-containing porphyrin nanosheets. *Microchim. Acta* **2022**, *189*, 108, doi:10.1007/s00604-022-05212-w.
83. Gazouli, M.; Liandris, E.; Andreadou, M.; Sechi, L.A.; Masala, S.; Paccagnini, D.; Ikonopoulou, J. Specific detection of unamplified mycobacterial DNA by use of fluorescent semiconductor quantum dots and magnetic beads. *J. Clin. Microbiol.* **2010**, *48*, 2830–2835, doi:10.1128/JCM.00185-10.
84. Cimaglia, F.; Aliverti, A.; Chiesa, M.; Poltronieri, P.; De Lorenzis, E.; Santino, A.; Sechi, L.A. Quantum dots nanoparticle-based lateral flow assay for rapid detection of mycobacterium species using anti-FprA antibodies. *Nanotechnol. Dev.* **2012**, *2*, 5, doi:10.4081/nd.2012.e5.
85. Jiang, X.; Zeng, H.; Duan, C.; Hu, Q.; Wu, Q.; Yu, Y.; Yang, X. One-pot synthesis of stable and functional hydrophilic CsPbBr<sub>3</sub> perovskite quantum dots for “turn-on” fluorescence detection of *Mycobacterium tuberculosis*. *Dalton Trans.* **2022**, *51*, 3581–3589, doi:10.1039/D1DT03624F.
86. Mohd Bakhori, N.; Yusof, N.A.; Abdullah, J.; Wasoh, H.; Ab Rahman, S.K.; Abd Rahman, S.F. Surface enhanced CdSe/ZnS QD/SiNP electrochemical immunosensor for the detection of *Mycobacterium tuberculosis* by combination of CFP10-ESAT6 for better diagnostic specificity. *Materials* **2019**, *13*, 149, doi:10.3390/ma13010149.
87. Gliddon, H.D.; Kaforou, M.; Alikian, M.; Habgood-Coote, D.; Zhou, C.; Oni, T.; Anderson, S.T.; Brent, A.J.; Crampin, A.C.; Eley, B.; et al. Identification of reduced host transcriptomic signatures for tuberculosis disease and digital PCR-based validation and quantification. *Front. Immunol.* **2021**, *12*, 637164, doi:10.3389/fimmu.2021.637164.
88. Boyle, D.S.; McNerney, R.; Teng Low, H.; Leader, B.T.; Pérez-Osorio, A.C.; Meyer, J.C.; O’Sullivan, D.M.; Brooks, D.G.; Piepenburg, O.; Forrest, M.S. Rapid detection of *Mycobacterium tuberculosis* by recombinase polymerase amplification. *PLoS ONE* **2014**, *9*, e103091, doi:10.1371/journal.pone.0103091.
89. Verma, S.; Dubey, A.; Singh, P.; Tewerson, S.; Sharma, D. Adenosine deaminase (ADA) level in tubercular pleural effusion. *Lung India* **2008**, *25*, 109, doi:10.4103/0970-2113.44121.
90. DeVito, J.A.; Morris, S. Exploring the structure and function of the mycobacterial KatG protein using *trans*-dominant mutants. *Antimicrob. Agents Chemother.* **2003**, *47*, 188–195, doi:10.1128/AAC.47.1.188-195.2003.
91. Clifford, V.; Tebruegge, M.; Zufferey, C.; Germano, S.; Forbes, B.; Cosentino, L.; Matchett, E.; McBryde, E.; Eisen, D.; Robins-Browne, R.; et al. Cytokine biomarkers for the diagnosis of tuberculosis infection and disease in adults in a low prevalence setting. *Tuberculosis* **2019**, *114*, 91–102, doi:10.1016/j.tube.2018.08.011.
92. Zhou, B.; Hao, Y.; Chen, S.; Yang, P. A Quartz crystal microbalance modified with antibody-coated silver nanoparticles acting as mass signal amplifiers for real-time monitoring of three latent tuberculosis infection biomarkers. *Microchim. Acta* **2019**, *186*, 212, doi:10.1007/s00604-019-3319-7.

93. Parate, K.; Rangnekar, S.V.; Jing, D.; Mendivelso-Perez, D.L.; Ding, S.; Secor, E.B.; Smith, E.A.; Hostetter, J.M.; Hersam, M.C.; Claussen, J.C. Aerosol-jet-printed graphene immunosensor for label-free cytokine monitoring in serum. *ACS Appl. Mater. Interfaces* **2020**, *12*, 8592–8603, doi:10.1021/acscami.9b22183. 537-539
94. Renshaw, P.S.; Panagiotidou, P.; Whelan, A.; Gordon, S.V.; Hewinson, R.G.; Williamson, R.A.; Carr, M.D. Conclusive evidence that the major T-cell antigens of the *Mycobacterium tuberculosis* complex ESAT-6 and CFP-10 form a tight, 1:1 complex and characterization of the structural properties of ESAT-6, CFP-10, and the ESAT-6-CFP-10 complex. *Journal of Biological Chemistry* **2002**, *277*, 21598–21603, doi:10.1074/jbc.M201625200. 540-543
95. Welin, A.; Björnsdóttir, H.; Winther, M.; Christenson, K.; Oprea, T.; Karlsson, A.; Forsman, H.; Dahlgren, C.; Bylund, J. CFP-10 from *Mycobacterium tuberculosis* selectively activates human neutrophils through a pertussis toxin-sensitive chemotactic receptor. *Infect. Immun.* **2015**, *83*, 205–213, doi:10.1128/IAI.02493-14. 544-546
96. Chai, Q.; Wang, X.; Qiang, L.; Zhang, Y.; Ge, P.; Lu, Z.; Zhong, Y.; Li, B.; Wang, J.; Zhang, L.; et al. A *Mycobacterium tuberculosis* surface protein recruits ubiquitin to trigger host xenophagy. *Nat. Commun.* **2019**, *10*, 1973, doi:10.1038/s41467-019-09955-8. 547-548
97. P, M.; Ahmad, J.; Samal, J.; Sheikh, J.A.; Arora, S.K.; Khubaib, M.; Aggarwal, H.; Kumari, I.; Luthra, K.; Rahman, S.A.; et al. *Mycobacterium tuberculosis* specific protein Rv1509 evokes efficient innate and adaptive immune response indicative of protective Th1 immune signature. *Front. Immunol.* **2021**, *12*, 706081, doi:10.3389/fimmu.2021.706081. 549-551
98. Lakshmi Priya, T.; Gopinath, S.C.B.; Tang, T.-H. Biotin-streptavidin competition mediates sensitive detection of biomolecules in enzyme linked immunosorbent assay. *PLoS ONE* **2016**, *11*, e0151153, doi:10.1371/journal.pone.0151153. 552-553
99. Omar, R.A.; Verma, N.; Arora, P.K. Development of ESAT-6 based immunosensor for the detection of *Mycobacterium tuberculosis*. *Front. Immunol.* **2021**, *12*, 653853, doi:10.3389/fimmu.2021.653853. 554-555
100. Diouani, M.F.; Ouerghi, O.; Refai, A.; Belgacem, K.; Tlili, C.; Laouini, D.; Essafi, M. Detection of ESAT-6 by a label free miniature immuno-electrochemical biosensor as a diagnostic tool for tuberculosis. *Mater. Sci. Eng. C* **2017**, *74*, 465–470, doi:10.1016/j.msec.2016.12.051. 556-558
101. Arora, J.; Kumar, G.; Verma, A.; Bhalla, M.; Sarin, R.; Myneedu, V. Utility of MPT64 antigen detection for rapid confirmation of *Mycobacterium tuberculosis* complex. *J. Global Infect. Dis.* **2015**, *7*, 66, doi:10.4103/0974-777X.154443. 559-560
102. Saengdee, P.; Chaisriratanakul, W.; Bunjongpru, W.; Sripumkhai, W.; Srisuwan, A.; Hruanun, C.; Poyai, A.; Phunpae, P.; Pata, S.; Jeamsaksiri, W.; et al. A silicon nitride ISFET based immunosensor for Ag85B detection of tuberculosis. *Analyst* **2016**, *141*, 5767–5775, doi:10.1039/C6AN00568C. 561-563
103. Xu, J.-N.; Chen, J.-P.; Chen, D.-L. Serodiagnosis efficacy and immunogenicity of the fusion protein of *Mycobacterium tuberculosis* composed of the 10-kilodalton culture filtrate protein, ESAT-6, and the extracellular domain fragment of PPE68. *Clin. Vaccine Immunol.* **2012**, *19*, 536–544, doi:10.1128/CVI.05708-11. 564-566
104. Wang, Q.; Boshoff, H.I.M.; Harrison, J.R.; Ray, P.C.; Green, S.R.; Wyatt, P.G.; Barry, C.E. PE/PPE proteins mediate nutrient transport across the outer membrane of *Mycobacterium tuberculosis*. *Science* **2020**, *367*, 1147–1151, doi:10.1126/science.aav5912. 567-568
105. García, J.; Puentes, A.; Rodríguez, L.; Ocampo, M.; Curtidor, H.; Vera, R.; Lopez, R.; Valbuena, J.; Cortes, J.; Vanegas, M.; et al. *Mycobacterium tuberculosis* Rv2536 protein implicated in specific binding to human cell lines. *Protein Sci.* **2005**, *14*, 2236–2245, doi:10.1110/ps.051526305. 569-571
106. Shirshikov, F.V.; Bespyatykh, J.A. TB-ISATEST: A diagnostic LAMP assay for differentiation of *Mycobacterium tuberculosis*. *Rus. J. Bioorg. Chem.* **2023**, *49*, 1279–1292, doi:10.1134/S1068162023060080. 572-573
107. Jaccottet, P.S.; Bothamley, G.H.; Batra, H.V.; Mistry, A.; Young, D.B.; Ivanyi, J. Specificity of antibodies to immunodominant mycobacterial antigens in pulmonary tuberculosis. *J. Clin. Microbiol.* **1988**, *26*, 2313–2318, doi:10.1128/jcm.26.11.2313-2318.1988. 574-575
108. Verbon, A.; Hartskeerl, R.A.; Moreno, C.; Kolk, A.H.J. Characterization of B cell epitopes on the 16K antigen of *Mycobacterium tuberculosis*. *Clin. Exp. Immunol.* **2008**, *89*, 395–401, doi:10.1111/j.1365-2249.1992.tb06969.x. 576-577



109. Salata, R.A.; Sanson, A.J.; Malhotra, I.J.; Wiker, H.G.; Harboe, M.; Phillips, N.B.; Daniel, T.M. Purification and characterization of the 30,000 dalton native antigen of *Mycobacterium tuberculosis* and characterization of six monoclonal antibodies reactive with a major epitope of this antigen. *J. Lab. Clin. Med.* **1991**, *118*, 589–598.
110. Andersen, A.B.; Hansen, E.B. Structure and mapping of antigenic domains of protein antigen b, a 38,000-molecular-weight protein of *Mycobacterium tuberculosis*. *Infect. Immun.* **1989**, *57*, 2481–2488, doi:10.1128/iai.57.8.2481-2488.1989.
111. Attallah, A.M.; Osman, S.; Saad, A.; Omran, M.; Ismail, H.; Ibrahim, G.; Abo-Naglla, A. Application of a circulating antigen detection immunoassay for laboratory diagnosis of extra-pulmonary and pulmonary tuberculosis. *Clin. Chim. Acta* **2005**, *356*, 58–66, doi:10.1016/j.cccn.2004.11.036.
112. Hunter, S.W.; Gaylord, H.; Brennan, P.J. Structure and antigenicity of the phosphorylated lipopolysaccharide antigens from the leprosy and tubercle bacilli. *J. Biol. Chem.* **1986**, *261*, 12345–12351.
113. Cocito, C.; Vanlinden, F. Preparation and properties of antigen 60 from *Mycobacterium bovis* BCG. *Clin. Exp. Immunol.* **1986**, *66*, 262–272.
114. Hendrickson, R.C.; Douglass, J.F.; Reynolds, L.D.; McNeill, P.D.; Carter, D.; Reed, S.G.; Houghton, R.L. Mass spectrometric identification of Mtb81, a novel serological marker for tuberculosis. *J. Clin. Microbiol.* **2000**, *38*, 2354–2361, doi:10.1128/JCM.38.6.2354-2361.2000.
115. Arend, S.M.; Ottenhoff, T.H.; Andersen, P.; van Dissel, J.T. Uncommon presentations of tuberculosis: The potential value of a novel diagnostic assay based on the *Mycobacterium tuberculosis*-specific antigens ESAT-6 and CFP-10. *Int. J. Tuberc. Lung Dis.* **2001**, *5*, 680–686.
116. Wilkinson, S.T.; Vanpatten, K.A.; Fernandez, D.R.; Brunhoeber, P.; Garsha, K.E.; Glinsmann-Gibson, B.J.; Grogan, T.M.; Teruya-Feldstein, J.; Rimsza, L.M. Partial plasma cell differentiation as a mechanism of lost major histocompatibility complex class II expression in diffuse large B-cell lymphoma. *Blood* **2012**, *119*, 1459–1467, doi:10.1182/blood-2011-07-363820.

**Disclaimer/Publisher’s Note:** The statements, opinions and data contained in all publications are solely those of the individual author(s) and contributor(s) and not of MDPI and/or the editor(s). MDPI and/or the editor(s) disclaim responsibility for any injury to people or property resulting from any ideas, methods, instructions or products referred to in the content.